The Net Advective Effect of a Vertically Sheared Current on a Coherent Vortex

FRÉDÉRIC VANDERMEIRSCH AND YVES MOREL

Service Hydrographique et Océanographique de la Marine, Centre Militaire d'Océanographie, Brest, France

GEORGI SUTYRIN

Graduate School of Oceanography, University of Rhode Island, Narragansett, Rhode Island

(Manuscript received 19 October 1999, in final form 31 October 2000)

ABSTRACT

The nonlinear interaction of a localized vortex with a vertically sheared mean flow has been studied using numerical and asymptotic methods in a multilayer quasigeostrophic model on the beta plane.

Numerical solutions indicate that baroclinic large-scale flows have a weak influence on the translation of coherent vortices, even when the advective effect of the mean flow is important. This is opposed to what is observed in general for the dynamics of linear Rossby waves, which are sensitive to the presence of a baroclinic current. Thus, the nonlinear nature of vortices has to be taken into account to explain this reduction of the net advective effect of a vertically sheared current on a coherent vortex.

The asymptotic method of Sutyrin and Morel is generalized to describe analytically the development of the beta gyres and corresponding vortex motion in the presence of a vertically sheared current. The initial vortex structure is prescribed as a piecewise constant potential vorticity anomaly in one or two layers with no motion in the lower layer. Three major effects are shown to contribute to the vortex translation: advection by the mean current, beta-gyre development due to planetary and mean flow potential vorticity gradients, and deformation of the vortex core. The analytical model predicts that the initial uniform gradient associated with the background current is strongly distorted and eventually ''homogenized,'' leading to the cancellation of the current net advective effect. In other words, the part of beta gyres associated with the mean-flow potential vorticity gradient compensates most of the advection by the baroclinic part of the current. Thus, the vortex is advected mainly by the planetary beta gyres (and the barotropic part of the flow if any).

The influence of the vortex size and strength on this compensation mechanism is evaluated.

1. Introduction

Long-lived rings and submesoscale coherent vortices (SCV) are found in all seas and oceans and their influence on transport of scalar properties and large-scale circulation is well admitted (see McWilliams 1985; Olson 1991). A number of hydrographic cruises have been recently devoted to explore intense oceanic vortices such as rings of the Gulf Stream or Agulhas Current (see, among many others, Olson 1980; Joyce and McDougall 1992; Olson and Evans 1986; van Ballegooyen et al. 1994), Slope Water or Mediterranean Water eddies (see Pingree and Le Cann 1992, 1993a,b, 1994; Armi et al. 1989; Richardson et al. 1989; Chérubin et al. 1997; Paillet et al. 1999), and other vortex types. These observations elucidated many features of the dynamics of rings and SCVs, which stimulated numerical and analytical studies.

Corresponding author address: Dr. Yves Morel, Service Hydrographique et Océanographie de la Marine (EPSHOM-CMO), Centre Militaire d'Océanographie, B.P. 426, 29275 Brest Cedex, France.
E-mail: morel@shom.fr

In this paper we focus on the propagation of SCVs that has been the subject of many investigations (see Morel 1995a; Morel and McWilliams 1997, and references therein). On the spherical earth for instance, it is well known that oceanic vortices are strongly influenced by a barotropic potential vorticity (PV) gradient called the planetary β effect. Rotational advection of the background PV by the vortex swirling flow produces dipolar secondary circulations (called beta gyres), which lead to a self-propagation of the whole structure relative to the surrounding flow (see McWilliams and Flierl 1979; Sutyrin 1987).

Other mechanisms exist that can affect the propagation of vortices, such as bottom topography or background currents. Under the influence of a constant barotropic current, vortices are merely advected at the current velocity. The advection speed associated with a vertically sheared background current has been calculated by Hogg and Stommel (1990, hereafter HS) or Marshall and Parthasarathy (1993, hereafter MP). However, besides this direct advective effect on the vortex, a vertically sheared current is generally associated with a *baroclinic* PV gradient that results in modification of

the β gyres and induces an additional vortex displacement. Kaz'min and Sutyrin (1990) and Morel (1995a, hereafter M95) have shown that this effect, which we will refer to as ''*baroclinic* β effect'' because of its similarity with the planetary β effect, is important and could drastically modify the vortex trajectory.

This paper focuses on the net influence of a large-scale vertically sheared mean current on the propagation of coherent vortices, taking both advective and baroclinic β effect into account. In section 2, we discuss previous studies. In section 3, we present numerical solutions obtained with a quasigeostophic model. They show that the influence of a baroclinic large-scale current on the propagation of SCVs is generally weak and that the baroclinic β effect opposes and inhibits the advective effect. We then show that the nonlinear nature of SCVs has to be taken into account to explain this compensation mechanism and develop a nonlinear analytical model in section 4. We show that this model indeed predicts compensation and yields a physical explanation for this mechanism (section 5). The influence of the vortex structure is studied in section 6 and we conclude in section 7.

2. Background

When an axisymmetric vortex evolves under the influence of a constant barotropic current, it is merely advected at the current speed. In nature, large-scale oceanic currents are usually decreasing with depth and it is thus important to take into account their baroclinic[1] component to evaluate their influence on the displacement of vortices. This effect is much more complicated than a simple advection.

Hogg and Stommel (1990) study the advective effect of a vertically sheared current on a vortex, the ocean is represented by two active layers above an infinite and resting lower layer (2½ reduced gravity model) with a constant mean current in the upper layer. The vortex is represented by two point vortices, one in each layer. The slope of interface between the layers due to the background current vertical shear and associated with the baroclinic β effect is neglected in HS calculations.

The point vortex in the upper layer is advected by the mean current. As both point vortices tend to trap each other, HS find that regimes exist in which the whole structure (e.g., both point vortices) is advected by the mean current and thus conclude that an upper thermocline large-scale current is able to advect a subsurface vortex, provided the latter has a PV signature up to the sea surface. As mentioned above, the propagation speed is not just equal to the upper-layer current speed. Indeed, the vortex structure deformation has to be taken into account (the current vertical shear tilts the vortex), the mean propagation speed is given by the displacement of the gravity center of the structure (e.g., the gravity center of the point vortices weighted by their respective strength) and can be easily derived from HS calculations. It is equal to the vertical average of the mean current weighted by the vortex PV structure [see morel (1995b) Eqs. (12)–(13) in HS],

$$U_{\text{prop}} = \frac{d_1 s_u U_u + d_2 s_m U_m}{d_1 s_u + d_2 s_m}, \tag{1}$$

with HS notations [(d_1, d_2), (s_u, s_m), and (U_u, U_m) are, respectively, the layer depths, point vortex strengths, and background current in the upper and middle layer]. In their paper, MP derive a similar result considering vortices with piecewise constant PV structures subject to the tearing effect of a baroclinic current [see their Eq. (26)].

As stated above, these models rely on the assumptions that the vortex has a PV signature up to the upper layer of the ocean and that the interface slope associated with the mean current vertical shear can be neglected. Morel (1995) used a three-layer quasigeostrophic model to show that the interface slope is associated with a background baroclinic PV gradient similar to the planetary β effect: the *baroclinic* β effect. This baroclinic β effect results in the development of beta gyres, which in turn induce a propagation of the vortex even when the vortex does not have a PV signature in the upper layer. The propagation speed was shown to be of the same order of magnitude as the one associated with the planetary β effect ($\simeq 1$ cm s^{-1}) for reasonable choices of the model parameters (stratification, background current vertical shear, and vortex structure).

Thus, when a vortex interacts with a baroclinic mean current, both the advective effect and baroclinic β effect can induce substantial propagation. It is thus interesting to study the resulting net advection and whether both effects are opposed or not.

3. Numerical solutions

Notice that because they used a reduced-gravity model, the background mean current in HS had no barotropic component. In fact, a barotropic constant mean current U_{Bt} would simply induce an additional displacement of the whole structure (at the speed U_{Bt}). In the rest of this study, we will therefore only consider baroclinic currents with no mean transport ($U_{\text{Bt}} = 0$).

a. The quasigeostrophic model

We restrict our investigations to quasigeostrophic dynamics, that is to say we only consider vortices associated with small Rossby numbers $U/fR = \Omega/f$ (where U, Ω, and R are respectively the vortex velocity, vorticity, and radius) and moderate isopycnal deviations. Taking into account the planetary β effect, the nondi-

[1] The barotropic part of a current U_{Bt} is here defined as its vertical average. A baroclinic current is a current with no barotropic component $U_{\text{Bt}} = 0$.

mensional equations of motion for a multilayer stratified fluid are associated with the conservation of the total potential vorticity $Q_k = PV_k + \beta y$ in each layer k and can be written (see Pedlosky 1987, chap. 6.16),

$$\partial_T \mathrm{PV}_k + J(\Psi_k, \mathrm{PV}_k) + \beta\partial_X\Psi_k = 0 \tag{2a}$$

$$\mathrm{PV}_k = \nabla^2\Psi_k + F_k^-(\Psi_{k-1} - \Psi_k) + F_k^+(\Psi_{k+1} - \Psi_k) \tag{2b}$$

$$F_k^+ = \frac{\rho_o f_o^2 R^2}{g(\rho_{k+1} - \rho_k)H_k} \qquad F_k^- = \frac{\rho_o f_o^2 R^2}{g(\rho_k - \rho_{k-1})H_k}, \tag{2c}$$

where $J(A, B) = \partial_X A\partial_Y B - \partial_X B\partial_Y A$ is the Jacobian of A and B, Ψ_k and PV_k are the nondimensional streamfunction and potential vorticity anomaly in the kth layer, T is the time, X and Y are the eastward and poleward coordinates, f_o the Coriolis frequency, and H_k and ρ_k the layer depth at rest and density of the kth layer. Here $\beta = \beta^{\mathrm{dim}} R/\Omega$ is the nondimensional β coefficient, which is assumed to be small for strong vortices. To account for upper and lower boundary conditions, we also impose $F_1^- = 0$ and $F_N^+ = 0$ where N is the number of active layers.[2]

We now take into account a mean large-scale current that is constant in each layer but vertically sheared. For the sake of simplicity we only consider zonal currents, but our results can be generalized to nonzonal currents provided the meridional component is chosen so that (2a) is verified. If U_k is the zonal large-scale current in layer k, Eq. (2a) becomes (see M95)

$$\partial_T \mathrm{PV}_k + U_k\partial_X \mathrm{PV}_k + J(\Psi_k, \mathrm{PV}_k) + (\beta + \beta_k^U)\partial_X\Psi_k = 0 \tag{3a}$$

$$\beta_k^U = -F_k^+(U_{k+1} - U_k) - F_k^-(U_{k-1} - U_k), \tag{3b}$$

where Ψ_k and PV_k now represent an anomaly with respect to the mean current and will be associated with a vortex in the rest of this study. β_k^U represents the background current PV gradient and does not depend on horizontal coordinates. It is added to the planetary β effect so that we can define the total beta coefficient in each layer $\beta_k^t = \beta + \beta_k^U$.

b. Results

In M95 the number of layers was small, and we here choose to repeat the experiments with a 10-layer quasigeostrophic model where we consider a purely baroclinic mean current and different vortex structures. The model is a pseudospectral code and is described in Dewar and Flierl (1987), and we here present the results in dimensional quantities. The domain is square and biperiodic with a width of 600 km and a 128 × 128 horizontal grid giving a grid size $\Delta x \simeq 4.7$ km. The planetary β effect is taken into account with $\beta = 2 \times 10^{-11}$ s^{-1} m^{-1}, the Coriolis parameter is $f = 7.5 \times 10^{-5}$ s^{-1}, and a biharmonic dissipation of vorticity is used with a viscosity coefficient of $\nu = 10^8$ m^4 s^{-1} to marginally avoid computationnal instability. Figure 1 gives the background stratification and current structure. The latter is intensified in the upper part of the ocean decreasing from 1 cm s^{-1} at the surface to 0 cm s^{-1} at 1000-m depth and with a moderate ($\simeq$0.3 cm s^{-1}) countercurrent below. The fluid is divided into 10 layers of equal depth ($H = 300$ m) and the density jumps are associated with the stratification given in Fig. 1. A first internal radius of deformation $R_d \simeq 30$ km has been calculated from these parameters. The initial streamfunction associated with the vortex is chosen as in Morel and McWilliams (1997),

$$\Psi = e^{-r^2/R^2} F(z) \tag{4}$$

with

$$F(z) = \begin{cases} \exp\left[-\left(\dfrac{z - z_1}{H_s}\right)^2\right], & 0 \geq z \geq z_1 \\ 1, & z_1 \geq z \geq z_2 \\ \exp\left[-\left(\dfrac{z - z_2}{H_s}\right)^2\right], & z_2 \geq z \geq z_{\mathrm{bottom}}. \end{cases} \tag{5}$$

We now compare the evolution of vortices on the planetary β plane to the evolution obtained with the additional effect of the background current. We also resume the latter experiment taking only the advective effect of the current [e.g., we artificially set $\beta^U = 0$ in Eq. (3a)] to evaluate the respective influence of the advective and baroclinic β effects.

Many vortex structures were studied but we will only present two cases here (see Table 1), one for a vortex associated with a moderate vertical shear (case 1, $H_s = 800$ m) and one with a strong vertical shear (case 2, $H_s = 200$ m), as they are representative of the main vortex types (see Morel and McWilliams 1997).

Figure 2 shows the PV anomaly in the first layer after 200 days, respectively, for the vortex structure (1) in Table 1. The three panels correspond to the three different configurations mentioned above: planetary β plane (Fig. 2a), planetary β plane with the additional effect of the background current (Fig. 2b), and planetary β plane with only the advective effect of the background current (Fig. 2c).

Comparing Figs. 2a and 2c we see that the effect of advection is first to reduce the westward propagation of the vortex from 125 to 35 km. This is expected as the vortex PV anomaly is concentrated in the upper part of the ocean (between 0 and 800 m) where the current is strong and oriented eastward. The mean current over this depth range is $\simeq$0.5 cm s^{-1}, which yields a mean displacement of $\simeq$90 km during 200 days, corresponding to the difference in the final zonal position. There

[2] We will also alternatively use $\Psi_N{}^+{}_1 = 0$ for reduced gravity configurations in which there is no barotropic mode.

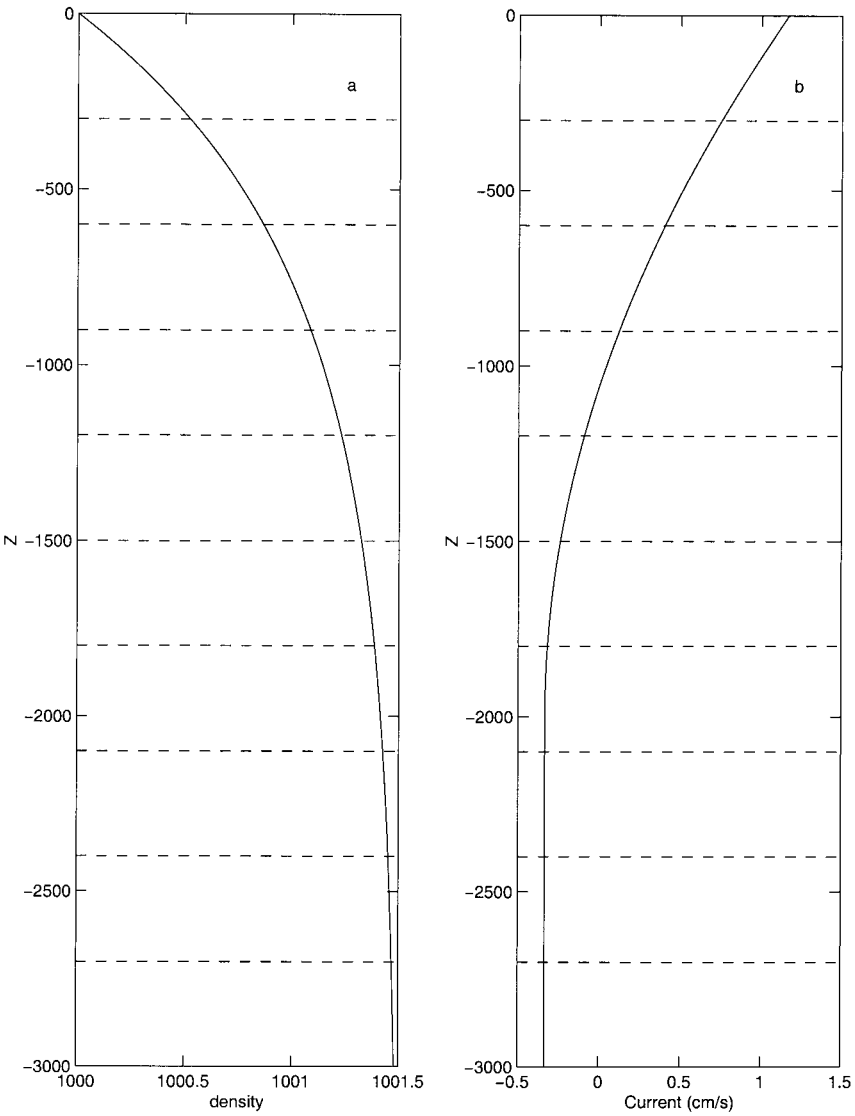

FIG. 1. Background stratification (a) and baroclinic current profile (b) for the 10-layer numerical experiments. The layer positions are also indicated with dashed lines.

is also a strong difference in the meridional displacement (160 km southward for Fig. 2a and 110 km for Fig. 2c), which is attributed to the current influence on the vortex deformation.

These differences are drastically reduced when the baroclinic β effect of the current is taken into account (see Fig. 2b). Indeed, the final position of the vortex in Fig. 2b is now pretty close to the pure β plane case in Fig. 2a: the zonal position difference is now only 50 km and the meridional position is almost exactly the same. This seems to indicate that the baroclinic β effect tends to compensate the advective effect of the current.

This is even clearer for the second vortex structure (case 2 in Table 1), corresponding to a vortex with a strong vertical shear. In this case, as opposed to the previous experiment, the vortex is baroclinically unstable. The initial instability phase yields to the rearrangement of the structure into a baroclinic dipole, or heton, that drastically influences the displacement. On the planetary β plane, the vortex trajectory now exhibits strong irregularities with loops, cusps, and stagnation phases (see Morel and McWilliams 1997). For such structures, modest changes during the evolution can lead to drastically different trajectories, and we therefore expect the changes induced by the background current to be en-

TABLE 1. Vortex structure for the 10 layer experiments where Z_c is the depth of the vortex core and Z_{th} is its thickness.

No.	R (in km)	$Z_c = (z_1 + z_2)/2$	$Z_{th} = (z_1 - z_2)$	H_s
1	30	0	0	800
2	60	150	600	200

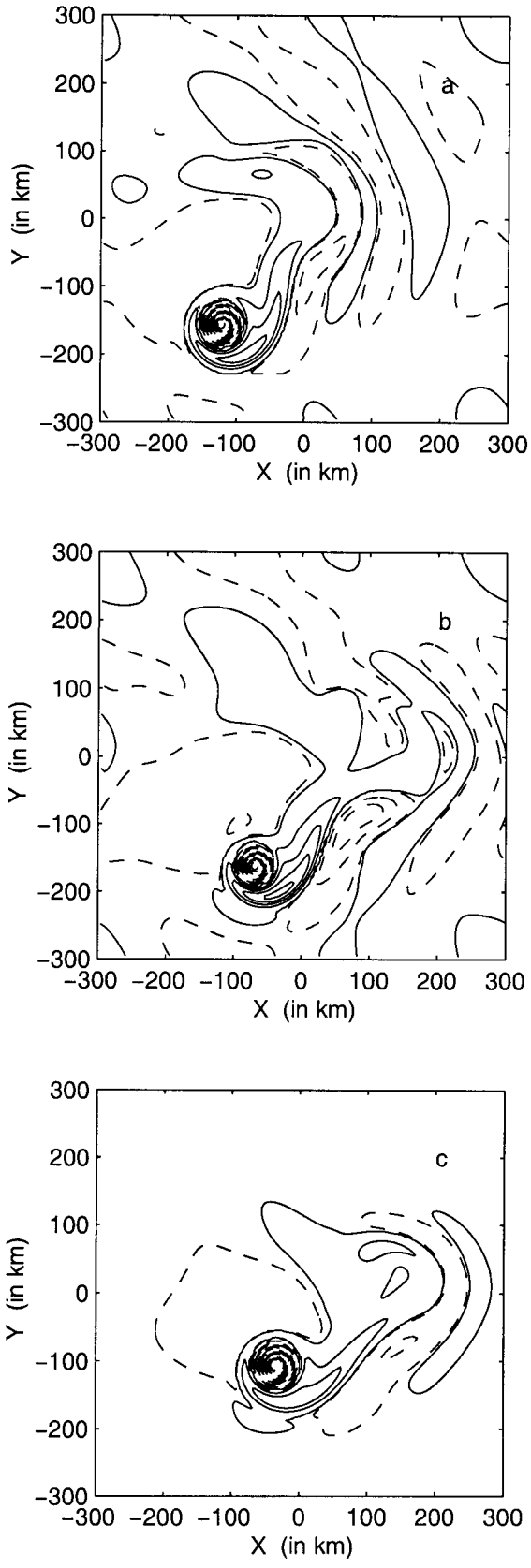

hanced. Figure 3 shows the PV anomaly in the first layer after 100 days for three different configurations: planetary β plane (Fig. 3a), planetary β plane with the additional effect of the background current (Fig. 3b), and planetary β plane with only the advective effect of the background current (Fig. 3c).

As mentioned above, for such initial PV structure, the addition of the current advective effect leads to drastically different trajectories and Figs. 3a and 3c exhibit very different results. In this respect, the similarity between Figs. 3a and 3b is striking and surprising as one would expect the addition of a complex process, such as the development of the baroclinic β gyre, to yield even stronger differences. In this case again we conclude that the baroclinic β effect compensates most of the changes associated with the advective effect of the background current.

Different vortex structures [radius R and vertical scales (Z_c, Z_{th}, H_s)] have been tested. They all confirmed our conclusion: for large-scale purely baroclinic currents, advection is always partly compensated by the baroclinic β effect. The meridional and zonal displacements induced by advection are in general reduced by 30%–95%.

4. Analytical model

a. Is compensation a linear mechanism?

The weak influence of a baroclinic large-scale current on the dynamics of a vortex seems associated with the compensation of advection by the baroclinic β effect. To explain this compensation mechanism, we can first examine the influence of a baroclinic current on the propagation of linear Rossby waves, especially long waves as—on the planetary β plane—the displacement speed of vortices is known to be close to the propagation speed of long Rossby waves (see McWilliams and Flierl 1979; Sutyrin and Flierl 1994).

In fact, both observations and theoretical results show that linear Rossby waves are pretty sensitive to the presence of a large-scale baroclinic current and even though both advection and baroclinic β effect can alter the propagation speed of Rossby waves, both effects do not generally compensate for linear waves. A detailed analysis of this topic can be found in Dewar (1998) or De Szoeke and Chelton (1999). We here restrict our demonstration to the following three arguments:

1) Dewar (1998) and De Szoeke and Chelton (1999)

←

FIG. 2. First-layer PV anomaly for the vortex structure 1 in Table 1 at time $t = 200$ days for an evolution on the planetary β plane (a), taking the background current into account (b), and with the current but neglecting the baroclinic β effect due to the background current (c). Notice the final vortex position is roughly similar between (a) and (b) whereas in (c) the vortex zonal and meridional displacement is weaker.

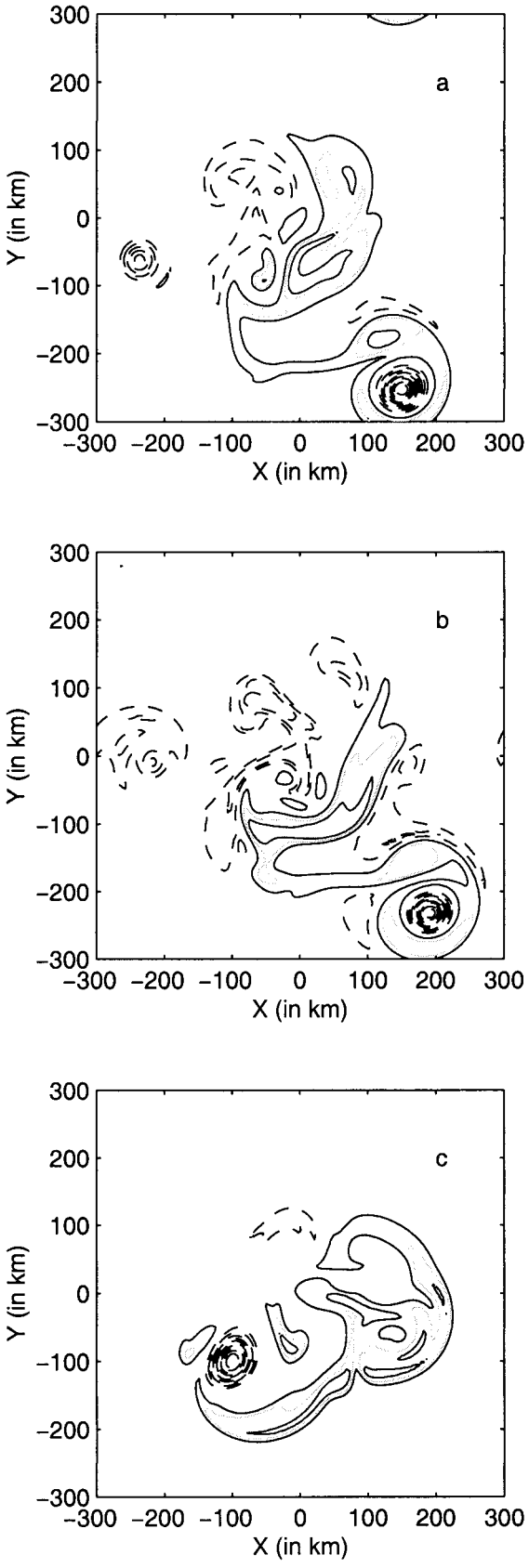

have shown that advection of Rossby waves by a large-scale baroclinic current is not compensated by the baroclinic β effect in general. Both effects can be complementary and accelerate the propagation speed to the west. Their results explain the observed long Rossby wave propagation in nature, which is "too fast" to be associated with the pure planetary β-plane effect.

2) It is also particularly interesting to notice that even though the vortex dynamics are pretty similar, the Rossby wave patterns in Figs. 2a and 2b (or Figs. 3a and 3b) are very different.
3) Finally, we will see below (section 5b) that the compensation mechanism is associated with the vortex ability to distort the background PV field, which is the feature of nonlinear perturbations. This is not the case for linear Rossby waves; on the contrary waves are dispersed by the background field.

Therefore the observed systematic compensation for vortices has to be linked to their nonlinear nature.

b. Nonlinear asymptotic solutions

1) ANALYTICAL RESULTS

Equation (3a) is too complicated to be solved in the general case for the evolution of a vortex because of the Jacobian nonlinear term, and it is not possible to find exact analytical solutions for the vortex translation. However, for an intense vortex on the β plane, an approximate analytic solution has been suggested for early stages (several vortex turnover periods) of vortex evolution by Reznik and Dewar (1994) for a barotropic model and Sutyrin and Flierl (1994) for a reduced gravity model. The latter has recently been generalized by Sutyrin and Morel (1997, hereafter SM) for a multilayer quasigeostrophic model.

The Sutyrin and Morel model calculates both the baroclinic β and vortex deformation effects on the propagation speed of the structure, and comparisons with numerical results show very good agreement up to several or even tens of vortex turnover timescales in general (see SM). It is based on different assumptions that are valid during the early stages of the evolution:

1) Intense vortices (for which $\max|\beta_k^t| = \max|(\beta_k^t)^{\dim} R/\Omega| \ll 1$) conserve their axisymmetric velocity field (in the reference frame moving with the vortex).
2) The development of the beta gyres is associated with the deformation of the background PV field by the

←

FIG. 3. First-layer PV anomaly for the vortex structure 2 in Table 1 at time $t = 100$ days for an evolution on the planetary β plane (a), taking the background current into account (b), and with the current but neglecting the baroclinic β effect (c). Notice the similarity of (a) and (b) and their strong difference with (c).

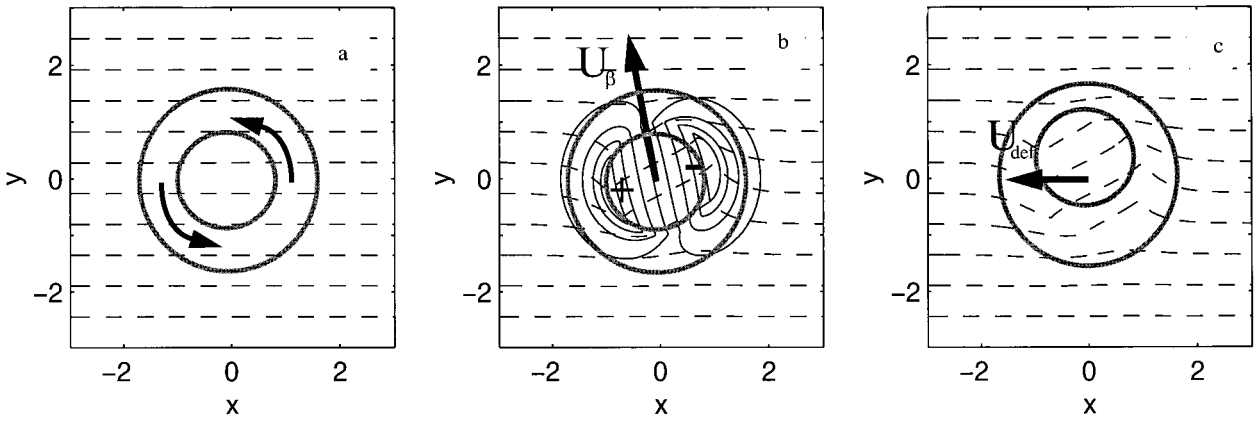

FIG. 4. This plot illustrates both the beta-gyre development and deformation effects for the propagation of a strong vortex on the β plane. The dipolar planetary PV field is represented by dashed lines and the (cyclonic) vortex is materialized by thick gray circular contours (two contours are shown to account for the vortex deformation effect). The initial planetary PV field (a) is first distorted by the symmetric vortex circulation (b). The difference between the deformed and the initial PV fields [thin plain lines in b) represents a PV anomaly associated with a dipolar circulation, the beta gyre, which entails the vortex propagation (U_β). This secondary circulation also modifies the vortex structure and (c) the initially concentric contours representing the vortex are put out of center. This deformation also induces a self-propagation of the vortex (U_{def}). Note that for a cyclonic vortex, the dipolar PV anomaly, associated with the beta gyre, is positive (negative) in the western (eastern) side of the vortex as, in this side, particles from north (south) with a high (low) PV value are displaced southward (northward) where the planetary PV field is weaker (stronger). Such a dipolar pattern is associated with a northward current in the vortex core.

initial symmetric circulation (see Figs. 4a,b). This induces a dipolar velocity field that superposes on the symmetric circulation and sets off the vortex propagation.

3) The beta-gyre development induces a deformation of the vortex structure, which also modifies the vortex propagation (see Fig. 4c). To calculate the vortex deformation, SM consider vortices with piecewise constant PV structure so that the nonlinear term vanishes everywhere except along the vortex PV contours, which permits an explicit calculation for the early stages.

We have extended SM to take into account the effect of a large-scale background current. The analytical derivation is given in appendix A and is similar to SM. Even though the asymptotic model can be derived in a general case with as many PV contours for the vortex as wanted, the results of the calculations can be interpreted more easily if we only consider two PV contours located in layers, say k_1 and k_2, with respective radii r_1 and r_2 and strength Δ_1 and Δ_2. This special case will also permit a closer comparison with HS and M95. If the vortex center is defined to be the center of the first PV (in layer k_1) contour, the eastward and northward vortex center translation velocity $\mathbf{u} = (U, V)$ can then be written

$$\mathbf{u} = \mathbf{u}_{\text{adv}} + \mathbf{u}_\beta + \mathbf{u}_\beta^{\text{def}}$$

or in complex form

$$U + iV = U_{\text{adv}} + iV_{\text{adv}} + U_\beta + iV_\beta + U_\beta^{\text{def}} + iV_\beta^{\text{def}}, \tag{6}$$

where $\mathbf{u}_{\text{adv}}$ is similar to the advective effect found by HS and MP, and for which the effect of the vortex core deformation has been taken into account. Here $\mathbf{u}_\beta$ represents the translation associated with the development of the total beta gyres (i.e., planetary and baroclinic β, see Fig. 4b) and $\mathbf{u}_\beta^{\text{def}}$ describes the additional effect of the vortex core deformation induced by the latter (see Fig. 4c). Both terms were neglected in previous analytical calculations.

We now detail and analyze each of these three terms with

$$\begin{aligned}\mathbf{u}_{\text{adv}} &\equiv U_{\text{adv}} + iV_{\text{adv}} \\ &= U_{k1} + \frac{\sigma_1(U_{k2} - U_{k1})}{\sigma}(1 - e^{i\sigma t}) \qquad (7a)\\ \mathbf{u}_\beta &\equiv U_\beta + iV_\beta \\ &= \frac{1}{r_1}\sum_{n,k}(\beta_k^U + \beta)P_{k1}^{(n)}\alpha_k^{(n)} \\ &\quad \times \left[-\frac{r_1}{\gamma_n^2} - \int r\, dr G_1^{(n)}(r_1|r)e^{i\overline{\Omega}_k(r)t}\right] \qquad (7b)\\ \mathbf{u}_\beta^{\text{def}} &\equiv U_\beta^{\text{def}} + iV_\beta^{\text{def}} \\ &= -\sigma_1\sum_{n,k}(\beta_k^U + \beta)\alpha_k^{(n)}\int r\, dr \\ &\quad \times \left[\frac{P_{k1}^{(n)}}{r_1}G_1^{(n)}(r_1|r) - \frac{P_{k2}^{(n)}}{r_2}G_1^{(n)}(r_2|r)\right] \\ &\quad \times \left[\frac{e^{i\overline{\Omega}_k(r)t} - e^{i\sigma t}}{\overline{\Omega}_k(r) - \sigma} + \frac{1 - e^{i\sigma t}}{\sigma}\right] \qquad (7c)\end{aligned}$$

$$\overline{\Omega}_k(r) = -\frac{1}{r}\sum_n P_k^{(n)}[\alpha_{k1}^{(n)}\Delta_1 G_1^{(n)}(r\,|\,r_1) + \alpha_{k2}^{(n)}\Delta_2 G_1^{(n)}(r\,|\,r_2)] \quad (7d)$$

$$\sigma_1 = -\frac{1}{r_1}\sum_n P_{k1}^{(n)}\alpha_{k2}^{(n)}\Delta_2 G_1^{(n)}(r_1\,|\,r_2) \quad (7e)$$

$$\sigma_2 = -\frac{1}{r_2}\sum_n P_{k2}^{(n)}\alpha_{k1}^{(n)}\Delta_1 G_1^{(n)}(r_2\,|\,r_1) \quad (7f)$$

$$\sigma = \sigma_1 + \sigma_2. \quad (7g)$$

In these formulas, as in SM, (U, V) are the (eastward, poleward) components of the propagation velocity, $P^{(n)} = (P_1^{(n)}, \cdots P_k^{(n)}, \cdots, P_N^{(n)})$ is the nth vertical eigenmode associated with the stretching operator (see appendix A) and $-\gamma_n^2$ is its corresponding eigenvalue. The $N \times N$ matrix α with coefficients $\alpha_l^{(n)}$ is the inverse of the matrix P whose columns are the vectors $P^{(n)}$. Here $G_1^{(n)}$ is the Green function associated with the Helmholtz operator $[(r\partial_r(r\partial_r) - 1/r^2 - \gamma_n^2)]$, and is expressed in terms of modified Bessel functions K_1 and I_1 (see appendix A).

A few straightforward conclusions can be obtained from the analysis of Eqs. (7a–c). First, as the vortex is initially axisymmetric, $\mathbf{u}_\beta$ and $\mathbf{u}_\beta^{\text{def}}$ are initially null [it can indeed be shown that the terms in square brackets in Eq. (7b) cancel each other at $t = 0$] so that the initial translation speed is equal to U_{k1}, the background current in the layer of the vortex center.

Second, if the beta-gyre development is neglected, as said above, we recover HS and MP results described in section 2. Indeed, the time-independent term in (7a) is the equivalent of Eq. (1): the vortex translates at a propagation speed that is a vertical average of the background current weighted by the vortex PV structure, but also oscillates as soon as its structure is constituted of more than one contour [second term on the right-hand side of (7a)]. Notice that, if there is only one contour (e.g., if $\Delta_2 = 0$), then $\sigma_1 = 0$ and the vortex is simply advected by the current in the core layer (if the beta gyres are neglected).

Finally even though the effect of the beta gyres is initially null, notice that each term of the sums in (7b) and (7c) roughly have the same order of magnitude as the background current. Thus after an initial acceleration we expect the beta gyres to produce a strong influence on the vortex displacement.

Before analyzing the influence of the beta-gyre development and calculating the net advective effect of a baroclinic current, we briefly discuss the limits of the analytical model.

2) MODEL LIMITS

The general model limits are discussed in SM, and here we only discuss an additional problem associated with the fact that we take into account a background mean current, which can be unstable if $\beta + \beta_k^U$ changes sign in some layers. Indeed, the asymptotic model only considers the development of vortex perturbations of azimuthal mode one, which is in general the main perturbation induced by the background PV gradient, and the main source for the vortex translation. However, if the mean current is unstable, it can rapidly break into vortices that would interact with the initially isolated structure that we consider. In this situation, the latter will no longer propagate under the influence of a horizontally constant mean current and we expect the analytical model to have a reduced period of validity.

That is why we restrict our investigations to stable mean currents or at most slightly unstable ones with weak growth rates (see Vandermeirsch 1999). Taking the planetary β effect into account guarantees the stability of currents with moderate vertical shear [the Charney–Stern (1962), stability criterion indeed imposes that $\beta_k^U + \beta$ has the same sign in each layer].

Comparisons between numerical and analytical solutions (not shown) yield the same conclusion as in SM: the analytical predictions are very close to the numerical experiments up to at least a few vortex turnover times. The differences however grow with time, but the long time evolution tendency is generally well represented in our model, even for cases in which the background current is slightly unstable (see Vandermeirsch 1999).

5. Compensation mechanism

a. Compensation in the analytical solutions

Equations (7a–f) give the trajectory [a straightforward time integration of Eqs. (7a–c) gives us the vortex displacement] of the vortex center as a function of the background stratification, mean current, and vortex core structure. The model has been applied to different configurations, and we present the results obtained for a 2½ layer configuration with a stratification characterized by

$$F_1^+ = 5, \qquad F_2^- = 5, \qquad F_2^+ = 10$$

corresponding to nondimensional radius of deformation $r_{d1} = 0.58$ and $r_{d2} = 0.24$. The rotation rate $\overline{\Omega}$ is here chosen so that the nondimensional PV structure is $\Delta_1 = \Delta_2 = 1$. We also choose the length scale R so that the PV contour radii are $r_1 = r_2 = 1$. As in HS and MP, the PV contours are in different layers $k_1 = 1$ and $k_2 = 2$ (see Fig. 5). The planetary β effect is taken into account ($\beta = 0.1$). Different background current (U_1, U_2) and total β coefficients are examined and are given in table 2.

Figure 6 shows the vortex trajectories for 100 nondimensional time units [roughly corresponding to four vortex turnover times, $t_v = 2\pi/\max(\overline{\Omega}_1)$] and for case a and b in Table 2. The trajectory obtained with the numerical quasigeostrophic model are also shown (dashed lines) and we see that the analytic model closely

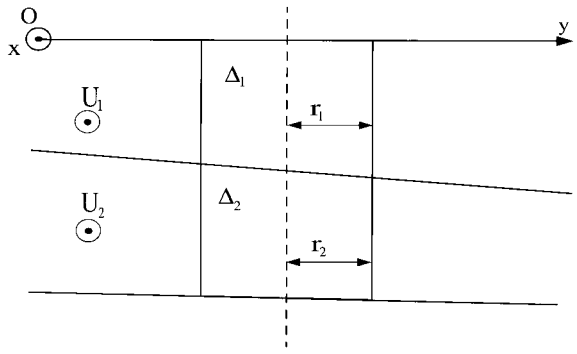

FIG. 5. Configuration used in the analytical model. We consider a 2½-layer model, with a vortex represented by two PV contours (one in each layer). The results we present are obtained with a vortex PV anomaly $\Delta_1 = \Delta_2 = 1$ and radii $r_1 = r_2 = 1$. Different background currents (U_1, U_2) were used.

describes the numerical solutions; even details of the trajectories (oscillations) are well reproduced.

The trajectories in Fig. 6 are associated with opposite sign (e.g., westward and eastward) background flows but are only slightly different. This demonstrates again the weak influence of the background current and the compensation of mean advection by the beta-gyre development. From Eq. (1), pure advection should indeed yield a final position difference $\Delta x \simeq 2$ instead of 0.3. This is underlined in Fig. 7 where we have presented the trajectory of cases b and c in Table 2. The latter is the same as case b but β^U is artificially neglected. As one can see by comparison between both trajectories the baroclinic β effect induces a westward propagation of the vortex and thus opposes and mostly compensates the eastward advective effect.

TABLE 2. Current structure and Δ_2 for each experiment ($\Delta_1 = 1$).

No.	Δ_2	U_1	U_2	β^U_1	β^U_2
a	1	−0.02	0	0	0.2
b	1	0.02	0	0.2	0
c	1	0.02	0	0.1	0.1

This compensation effect is, in fact, general. Indeed, in appendix B we demonstrate that for long time periods, the baroclinic beta gyre terms in (7b–c) exactly cancel the advective terms in (7a) so that, according to the analytical model, a baroclinic current has no net effect on the displacement of a coherent vortex.

However, as the analytical model is not valid for long time periods, this theoretical result bears some limitations. It demonstrates the systematic tendency of the baroclinic β effects to compensate advection, but compensation is not expected to be total in general.

b. Physical mechanism

As the analytical model developed above is able to reproduce the compensation of the advective effect of a current by the baroclinic β effect, it can also give us some insights on the physical mechanism.

For the sake of simplicity, let us omit the planetary β effect and focus on the effect of the baroclinic current. The beta-gyre development is associated with Eq. (7b), and as discussed above compensation is due to the vanishing influence of the integral in Eq. (7b). As the vortex deformation is a consequence of the beta-gyre development, we can focus on the latter process to explain the compensation mechanism.

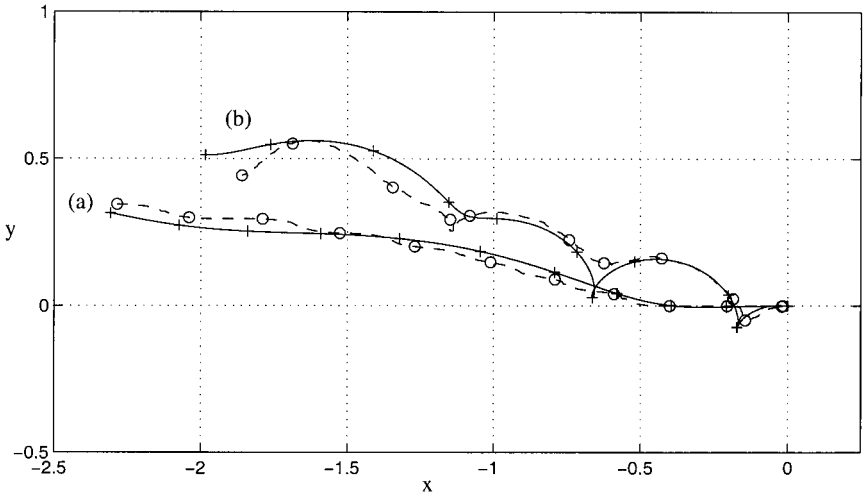

FIG. 6. Trajectories given by the analytical model (solid lines with crosses every 10 nondimensional time units) with the vortex structure described in Fig. 5, for different background currents and for 100 nondimensional time units (≃4 vortex turnover time). Trajectory (a) is obtained with a westward current, whereas trajectory (b) with an eastward current. Notice the final positions are not far apart. Trajectories obtained from a numerical quasigeostrophic model are also presented (dashed lines with circles every 10 nondimensional time units) to show the validity of the analytical calculations.

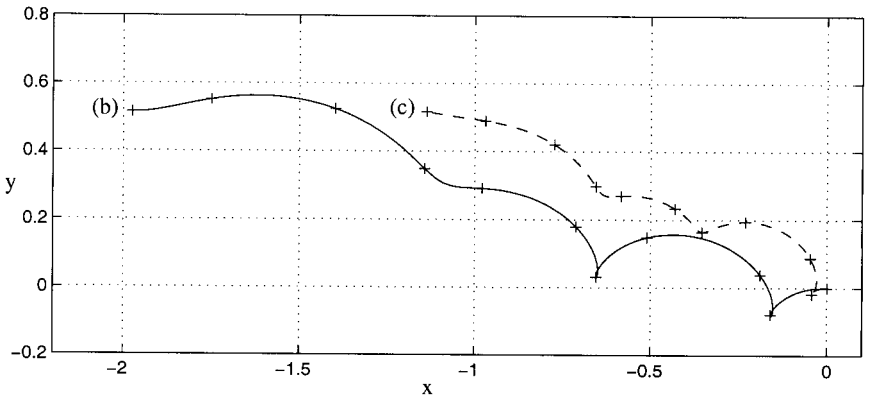

FIG. 7. Trajectories for configurations b (solid line) and c (dashed line) in Table 2. Both trajectories are obtained with the same configuration and a westward background current except the baroclinic β effect has been neglected for the dashed trajectory (e.g., $\beta^U \equiv 0$ in expt c). This underlines the influence of the baroclinic β effect, which compensates the eastward advection of the current.

As shown by the analytical calculations [see Eq. (A9) in appendix A] and discussed above, the beta-gyre development is—at first order and in our analytical model—a consequence of the deformation of the total dipolar PV field by the symmetric circulation. There is a direct correspondence between the total dipolar PV and the dipolar current responsible for the net vortex displacement. In particular, if the dipolar PV field vanishes, the propagation stops. This is illustrated in Fig. 8 where we have plotted the dipolar PV field at different times. Initially the beta-gyre is zero and has no effect, the simple PV shape is associated with the background current and the whole structure is merely advected at the background current speed (see Fig. 8a). The modification of the dipolar PV field by the symmetric circulation then changes the net advective effect (see Fig. 8b). To analyze the former and deduce the latter we follow Sutyrin and Flierl (1994) and split the domain into three different regions.

In the outer regions (zone III in Fig. 8c) $\overline{\Omega}$ is small so that the dipolar PV field and its contribution to the vortex displacement changes slowly. However, as shown in Fig. 8d, this region shrinks with time and its influence on the vortex propagation diminishes.

The intermediate region (zone II in Fig. 8c) corresponds to the transition between the core and the outer region. This area is strongly sheared as the rotation rate $\overline{\Omega}$ strongly varies. The PV field is strongly distorted and is rolled up into a spiral as shown in Sutyrin and Flierl (1994). This leads to the development of small-scale PV structure where opposite sign PV poles alternate along a vortex radius (see Figs. 8c,d). As the streamfunction or current field averages out the small-scale PV structure, the total dipolar circulation after a few vortex turnovers becomes weaker and weaker in the sheared region (this also means that the interface slope decreases with time). As the beta gyre homogenizes the dipolar PV field (or in other words, compensates the initial PV field associated with the background current), the contribution of this region to the vortex displacement rapidly vanishes. In addition, this area asymptotically spreads over the whole domain, which explains why compensation is total at large time in the analytical model.

In the vortex core (zone I in Fig. 8c) $\overline{\Omega}$ is strong but is almost constant (the core of vortices is indeed in near solid body rotation). The influence of this region on the vortex translation thus does not change in strength. However, the orientation of the PV gradient, and thus of the associated propagation speed, rotates with the vortex core (compare Figs. 8a, 8b, and 8c). This only adds an oscillation to the trajectory and has a weak effect on the displacement when averaged over a vortex turnover time.

Thus, even though the shear is pretty weak in some regions, the analytical model shows that because of PV homogenization in the sheared region (zone II) and the rapid solid body rotation of the core (zone I), we can expect a strong partial compensation of the advective effect by the baroclinic beta-gyre development at finite time. The compensation rate however depends on the outer region (zone III in Fig. 8c) extent and the rotation rate $\overline{\Omega}$. We therefore expect the process to be sensitive to the vortex size and strength and study their influence in the following section.

6. Influence of the vortex structure

Despite the limiting factors of our analytical model, as shown in Fig. 7 and confirmed in all our experiments, the compensation of the advective effect of a vertically sheared current by the baroclinic β effect is generally essential and well represented by the analytical solutions. We thus now use the latter to evaluate the sensitivity of the compensation mechanism on the vortex structure, in particular we want to study the influence of the core radius and vortex strength.

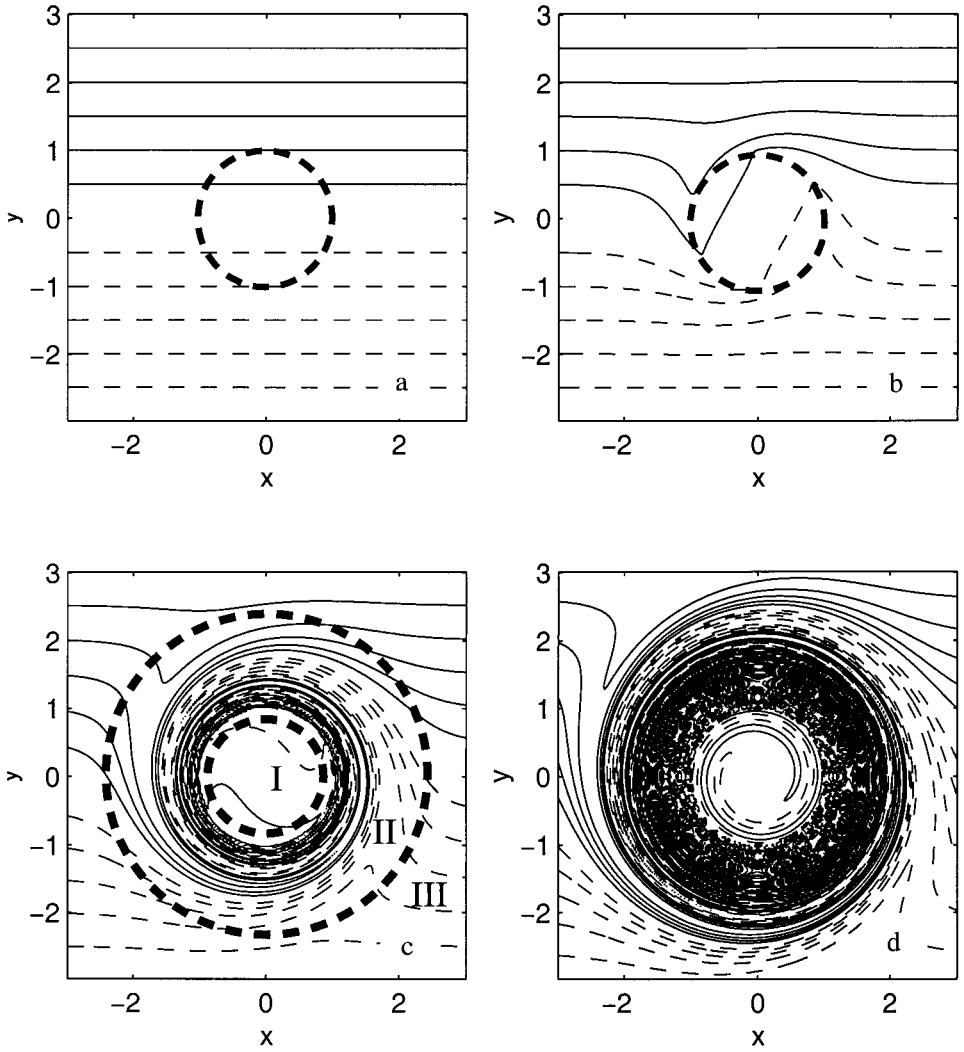

FIG. 8. Total dipolar PV field in the first layer for the vortex structure in Fig. 5 and at nondimensional time unit (a) $t = 0$, (b) $t = 5$, (c) $t = 100$, (corresponding to four vortex turnovers) and (d) $t = 1000$ (corresponding to 40 vortex turnovers). The vortex core is materialized by a thick dashed line. Notice the deformation of the PV field varies as there exists region with weak [zones I and III in (c)] and strong [zones II in (c)] horizontal shear. The distortion of the dipolar PV field leads to the development of a spiral structure where opposite sign PV alternate along a vortex radius (c). This structure slowly spreads over the whole domain (d) so that asymptotically the whole PV field is homogenized by this process. As a result the net velocity field associated with this PV structure becomes weaker and weaker, and the advective effect of the current is canceled.

To do so, we define the compensation rate

$$\tau = -\frac{X_{\beta^U}}{X_{\text{adv}}}, \tag{8}$$

where X_{β^U} and X_{adv} are given by Eqs. (7a–c) and represent the zonal displacement associated with the baroclinic β effect [corresponding to the terms proportional to β^U in (7b) and (7c)] and advective effect [corresponding to the terms given in (7a)], respectively. Here τ is positive if the baroclinic β gyres oppose the advective effect, and $\tau = 1$ if the compensation is total.

Figure 9 represents τ at a fixed time $t = 100 \approx 4t_v$ as a function of $s_1 = r_1/r_{d1}$, for the background stratification defined previously ($F_1^+ = F_2^- = 5$, $F_2^+ = 10$) and for an upper-layer mean current, $U_1 \neq 0$, $U_2 \neq 0$ (notice that τ does not depend on the mean current intensity). The plain line is associated with vortices constituted of one PV contour ($\Delta_1 = 1$, $\Delta_2 = 0$), and the dashed one with a two contour vortex ($\Delta_1 = 1$, $\Delta_2 = 1$). Note that for very small vortex radii, the compensation is close to zero, as argued in HS, and the baroclinic β effect is weak for small vortices. However, τ is always positive and generally increases with s_1 and for realistic vortex radii (in the ocean $s_1 \geq 1$) the com-

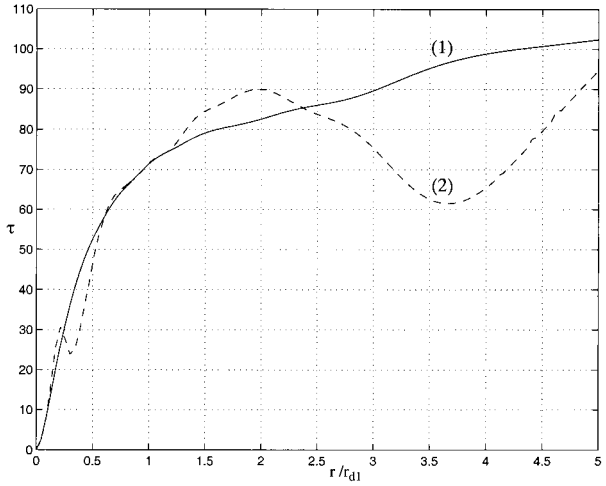

FIG. 9. Compensation rate τ in % as a function of $s_1 = r_1/r_{d1}$ and at $t = 100$. Here τ measures the compensation rate and is 100% when the baroclinic β effect exactly opposes the advection induced by the current. Notice that τ increases with the vortex size. For typical oceanic vortices, when $s_1 > 1$, the compensation reaches 60%–70%. The solid line is associated with a vortex core constituted of only one contour in the first layer ($\Delta_1 = 1$, $\Delta_2 = 0$) whereas the dashed one corresponds to a two-contour structure ($\Delta_1 = 1$, $\Delta_2 = 1$).

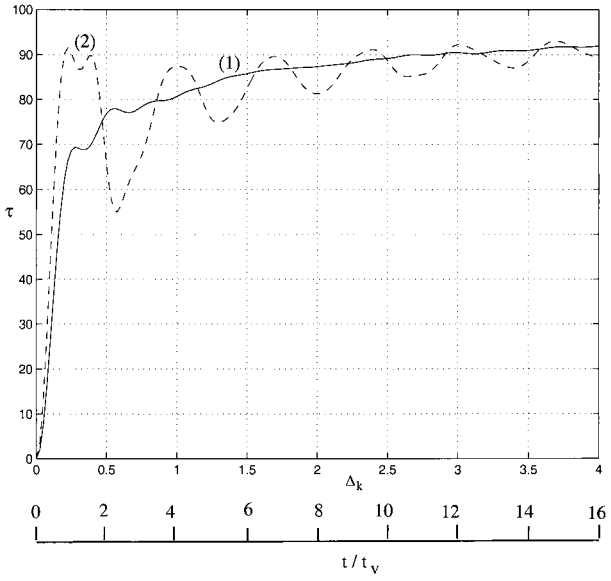

FIG. 10. Compensation rate τ in % as a function of the vortex strength Δ_k or equivalently the number of core rotations t/t_v. The solid line is again associated with a vortex having only one contour in the first layer ($\Delta_2 = 0$) whereas the dashed line corresponds to a two-contour structure ($\Delta_1 = \Delta_2$).

pensation is strong. This is expected: As argued in the previous section, compensation is associated with homogenization of PV in the vortex core. For a given rotation rate, the size of the homogenized region (which corresponds to the region in which the rotation rate is significant) increases with the vortex radius. Therefore, the larger the vortex, the stronger the compensation. The oscillation for the two-contour case is due to the oscillation associated with vertical tilting of the vortex core and is not thought to be significant on average.

Figure 10 is the same as Fig. 9 except that now the vortex radii are fixed ($r_1 = r_2 = 1$) and the vortex strength (Δ_1, Δ_2) is variable. Again, vortices with one and two contours are examined (in the latter configuration, both PV anomalies are located in different layers and have the same intensity). Notice that, because time has been nondimensionalized by the vortex rotation rate, increasing the vortex strength boils down to decreasing its turnover timescale, so that Fig. 10 can also be interpreted as the compensation rate sensitivity to the number of vortex turnovers (t/t_v). As in Fig. 9, τ is always positive and increases with the vortex strength or number of vortex turnovers; it exceeds 80% for $\Delta_k > 1$ (or four rotations of the vortex core). This result is expected as our analytical calculations show that compensation grows with the number of vortex turnovers. Also notice the oscillation for the two-contour case (dashed line), which, as in Fig. 9, is associated with the vortex core tilting and is not significant on average (it is damped at large time).

7. Conclusions

The main result of this study is that the advective effect of a large-scale baroclinic current is partly compensated by the beta-gyre development associated with the current potential vorticity gradient. This compensation can be total so that only the planetary β effect, hetonic interactions, and the barotropic part of the mean large-scale current are susceptible to induce a vortex propagation. Thus, we expect large-scale currents to have some effects on the translation of oceanic rings and SCVs only when the barotropic flow is significant.

This result has been demonstrated theoretically with an analytical model and numerically with a 10-layer model. The mechanism responsible for the compensation was also shown to be associated with the rolling up of the nonsymmetric dipolar PV structure by the symmetric vortex rotation in regions of strong horizontal shear and the solid body rotation of the vortex core. This highlights the nonlinear nature of the compensation mechanism: only coherent vortices can distort the background PV field. On the contrary, Rossby waves are dispersed by the latter, are unable to homogenize the background PV, and thus do not follow the same systematic compensation tendency. For the large-scale background currents and vortex structures considered, the compensation rate is between 30% and 95%. These quantitative results are probably sensitive to some parameters such as the vortex decay rate (Gaussian or exponential in this paper), but we believe our qualitative conclusions are robust. Indeed, as long as the vortex is

strong enough to deform the background PV field in some area, compensation should be effective.

It is interesting to notice that, in the numerical experiments, the assumptions of our analytical model were not always verified as, for instance, the vortex signature is sometimes small in some layers so that the vortex cannot be considered strong at these depths and its signal should be partly dispersed by the Rossby waves. In addition, the vortex deformation was sometimes strong and the trajectories greatly influenced by hetonic effects, which are not quantitatively well represented in our analytical model. Despite these violations of our assumptions, the main conclusion is still valid.

It is also worth mentioning that several observations at sea (Richardson et al. 1989; Kaz'min and Sutyrin 1990; Pingree and LeCann 1993; Paillet et al. 1999) have shown that floats released in the vicinity of vortices often exhibit drastically different trajectories than the floats trapped in their core. This shows that vortices are not advected by the surrounding currents, which is consistent with our results.

Other mechanisms can account for the observed vortex displacement, among which the planetary β effect probably has a major influence. As shown in Morel and McWilliams (1997), the latter effect can be drastically strengthened by hetonic self-propagation effects, and numerical experiments have demonstrated that realistic propagation speeds could be reached. Interaction with neighboring vortices, mesoscale currents (jets), or barotropic large-scale currents can obviously play a role too.

As mentioned earlier, the previous analytical model could be developed for meridional currents and the same results (compensation of meridional advection by the baroclinic β effect) would be obtained. However, meridional large-scale currents are known to be always unstable (see Pedlosky 1987, chap. 7.13) and we have therefore limited our study to stable zonal currents.

It is also important to emphasize that we only considered large-scale currents, that is to say background currents for which the horizontal shear at the vortex scale is negligible. In configurations with substantial background relative vorticity, associated with jets or eddies for instance, our results are not expected to be valid.

Acknowledgments. We first thank Drs. William Dewar and Glenn Flierl, who gracefully provided their QG pseudospectral model. Frédéric Vandermeirsch and Yves Morel are supported by the Service Hydrographique et Océanographique de la Marine (SHOM, French Navy Hydrographic and Oceanographic Service). Georgi Sutyrin is supported by the U.S. Office of Naval Research (Grant N000149710139) and by the National Science Foundation (Grant ATM-99 05209). This paper is a contribution to the SEMAPHORE and SEMANE research programs conducted by SHOM.

APPENDIX A

Derivation of the Analytical Model

Our goal here is to give some basic principles on which the analytical model relies and we refer to SM for details. In particular, for the sake of clarity and conciseness, we will not discuss here the theoretical validity of the present model, but rely on comparison with numerical experiments instead. The present calculations are, in fact, a straightforward generalization of SM that permits us to take a vertically sheared mean current into account.

The first step in solving (3a) for an initially axisymmetric vortex is to use cylindrical coordinates (r, θ) with the origin at the vortex center $r\cos\theta = X - X_0$, $r\sin\theta = Y - Y_0$, and to assume that the PV structure of the vortex is initially axisymmetric and piecewise constant.

Defining the propagation speed of the vortex $(U, V) = (\dot{X}_0, \dot{Y}_0)$, Eq. (3a) can be written

$$\partial_T \mathrm{PV}_k + J(\Psi_k + r[(U - U_k)\sin\theta - V\cos\theta], \mathrm{PV}_k) + \beta_k^t \partial_X \Psi_k = 0. \quad \text{(A1)}$$

Notice that in cylindrical coordinates $J(A, B) = 1/r(\partial_r A \partial_\theta B - \partial_r B \partial_\theta A)$. We then use the following splitting for the vortex streamfunction and PV

$$\Psi_k = \Phi_k + \phi_k \qquad \mathrm{PV}_k = Q_k + q_k, \quad \text{(A2)}$$

where Φ_k and Q_k are associated with the piecewise-constant potential vorticity part and verify

$$Q_k = \nabla^2\Phi_k + F_k^-(\Phi_{k-1} - \Phi_k) + F_k^+(\Phi_{k+1} - \Phi_k) = \sum_j \Delta_{k,j}\mathcal{H}(r_{k,j} + \eta_{k,j} - r), \quad \text{(A3)}$$

and ϕ_k is associated with the beta-gyre part of the PV q_k and verifies

$$q_k = \nabla^2\phi_k + F_k^-(\phi_{k-1} - \phi_k) + F_k^+(\phi_{k+1} - \phi_k). \quad \text{(A4)}$$

Here, $\mathcal{H}$ is the Heavyside function, $\Delta_{k,j} = Q_{k,j+1} - Q_{k,j}$ is the PV jump at the jth contour $r = r_{k,j} + \eta_{k,j}(\theta,t)$ in the kth layer, $r_{k,j}$ is its initial radius, and $\eta_{k,j}$ its deformation.

As gradients of Q_k give Dirac distributions, the splitting (A2) will permit us to separate the evolution of the vortex deformation $\eta_{k,j}$ and the beta-gyre development (associated with q_k). Using (A2)–(A4) in (A1) we get

$$\frac{\partial}{\partial t}\eta_{k,j} + \Omega_{k,j}\frac{\partial}{\partial\theta}\eta_{k,j} + \frac{1}{r_{k,j} + \eta_{k,j}}\frac{\partial}{\partial\theta}\Phi_{k,j} = -\frac{1}{r_{k,j} + \eta_{k,j}}\frac{\partial}{\partial\theta}(\phi_{k,j} + (U - U_k)r\sin\theta - Vr\cos\theta) \quad \text{(A5)}$$

with

$$\Omega_{k,j} = \frac{1}{r_{k,j} + \eta_{k,j}} \frac{\partial}{\partial r} \times (\Phi_{k,j} + \phi_{k,j} + (U - U_k)r \sin\theta - Vr\cos\theta),$$

and

$$\frac{\partial}{\partial t} q_k + J(\Phi_k + \phi_k + (U - U_k)r\sin\theta - Vr\cos\theta, q_k) = -\beta_k^t J(\phi_k + \Phi_k, r\sin\theta). \quad \text{(A6)}$$

Also, using (A1) and averaging azimuthally shows that at first order, the radially symmetric part of the vortex does not change. The next step is then to linearize (A5) and (A6), taking advantage of the fact that initially $\eta_{k,j} = 0$ and $\phi_{k,j} = 0$ and that both quantities should remain small for several Rossby wave periods (see SM for details). We thus split $\Phi_{k,j} = \overline{\Phi}_k(r) + \Phi'_k(r, \theta, t)$ where $\overline{\Phi}_k(r)$ is associated with the initial axisymmetric structure and verifies

$$\nabla^2\overline{\Phi}_k + F_k^-(\overline{\Phi}_{k-1} - \overline{\Phi}_k) + F_k^+(\overline{\Phi}_{k+1} - \overline{\Phi}_k) = \sum_j \Delta_{k,j}\mathcal{H}(r_{k,j} - r) \quad \text{(A7)}$$

and from which we derive the angular velocity

$$\overline{\Omega}_k = \frac{1}{r}\frac{d\overline{\Phi}_k}{dr}.$$

Subtracting (A7) from (A3) and linearizing then yields an equation for Φ'_k

$$\nabla^2\Phi'_k + F_k^-(\Phi'_{k-1} - \Phi'_k) + F_k^+(\Phi'_{k+1} - \Phi'_k) = \sum_j \Delta_{k,j}\eta_{k,j}\delta(r - r_{k,j}). \quad \text{(A8)}$$

Linearization of (A5)–(A6) then yields the following uncoupled equations:

$$\frac{\partial}{\partial t} q_k + \overline{\Omega}_k \frac{\partial}{\partial\theta} q_k = -\beta_k^t \overline{\Omega}_k r\cos\theta \quad \text{(A9)}$$

$$\frac{\partial}{\partial t}\eta_{k,j} + \overline{\Omega}_k\frac{\partial}{\partial\theta}\eta_{k,j} + \frac{1}{r_{k,j}}\frac{\partial}{\partial\theta}\Phi'_{k,j} = -\frac{1}{r_{k,j}}\frac{\partial}{\partial\theta}\phi_{k,j} - (U - U_k)\cos\theta - V\sin\theta. \quad \text{(A10)}$$

The last step is to solve Eq. (A4) and (A7)–(A10) for the azimuthal mode number one, which is the only source of propagation for our linearized analytical model. Equation (A9) is readily solved and yields $q_k = \beta_k^t[r\sin(\theta - \overline{\Omega}_k t) - r\sin\theta]$. Equations (A4), (A7), and (A8) are then similar to the PV inversion problem

$$\nabla_1^2\varphi_k + F_k^-(\varphi_{k-1} - \varphi_k) + F_k^+(\varphi_{k+1} - \varphi_k) = \Gamma_k \quad \text{(A11)}$$

with

$$\nabla_1^2 = \frac{1}{r}\frac{\partial}{\partial r} r\frac{\partial}{\partial r} - \frac{1}{r^2}.$$

This equation can be solved in terms of vertical modes $P^{(n)} = (P_1^{(n)}, \cdots, P_k^{(n)}, \cdots, P^{(n)})_N$ associated with the vortex stretching matrix defined by (2b, c) so that

$$F_k^-(P_{k-1}^{(n)} - P_k^{(n)}) + F_k^+(P_{k+1}^{(n)} - P_k^{(n)}) = -\gamma_n^2 P_k^{(n)}, \quad \text{(A12)}$$

where $\gamma_n^{-1} = R_n$ is the radius of deformation associated with the nth mode. We also define a matrix α, with coefficients $\alpha_k^{(n)}$, by orthogonality conditions with the vertical modes ($\Sigma_n \alpha_k^{(n)} P_1^{(n)} = \delta_{kl}$). Here α is the inverse of the matrix P whose columns are the eigenvectors $P^{(n)}$ (so that we also have $\Sigma_k \alpha_k^{(m)} P_k^{(n)} = \delta_{mn}$). Thus, if we set

$$\varphi_k = \sum_n \varphi^{(n)} P_k^{(n)} \quad \text{and} \quad \Gamma_k = \sum_n P_k^{(n)}\Gamma^{(n)},$$

then

$$\Gamma^{(n)} = \sum_l \alpha_l^{(n)}\Gamma_l$$

and $\varphi^{(n)}$ verifies

$$\nabla_1^2\varphi^{(n)} - \gamma_n^2\varphi^{(n)} = \Gamma^{(n)}.$$

A Green's function $G_1^{(n)}(r \mid r')$ for the Helmholtz's operator of the left-hand side [when $\Gamma^{(n)} = \delta(r' - r)$] is given by (see Abramowitz and Stegun 1970)

$$G_1^{(n)}(r|r') = \begin{cases} -r' I_1(\gamma_n r) K_1(\gamma_n r'), & r < r' \\ -r' I_1(\gamma_n r') K_1(\gamma_n r), & r > r' \end{cases}$$

with I_1 and K_1 being modified Bessel functions. For the flat bottom, rigid-lid case, a barotropic mode exists associated with $\gamma_0 = 0$. In that case $G_1^{(n)}(r \mid r')$ becomes

$$G_1^{(0)}(r|r') = \begin{cases} -\dfrac{r}{2}, & r < r' \\ -\dfrac{r'^2}{2r}, & r > r'. \end{cases}$$

The solution of (A11) is thus given by

$$\varphi_k(r) = \sum_{n,l} P_k^{(n)}\alpha_l^{(n)} \int G_1^{(n)}(r|r')\Gamma_l(r')\, dr'.$$

This permits inverting (A7), (A8), and (A9) and yields for (A10)

$$\frac{\partial}{\partial t}\eta_{k,j} - i\sum_{l,i} A_{k,j;l,i}\eta_{l,i} = i\frac{\phi_{k,j}}{r_{k,j}} - (U - U_k) - iV \quad \text{(A13)}$$

with

$$A_{k,j;l,i} = \overline{\Omega}_k(r_{k,j})\delta_{kl}\delta_{ij} + \frac{1}{r_{k,j}}\sum_n P_k^{(n)}\alpha_l^{(n)}\Delta_{l,i}G_1^{(n)}(r_{k,j}|r_{l,i}) \tag{A14}$$

$$\overline{\Omega}_k(r) = -\frac{1}{r}\sum_n P_k^{(n)}[\alpha_{k_1}^{(n)}\Delta_1 G_1^{(n)}(r|r_1) + \alpha_{k_2}^{(n)}\Delta_2 G_1^{(n)}(r|r_2)] \tag{A15}$$

$$\phi_{k,j} = i\sum_{n,l}\beta_l^t P_k^{(n)}\alpha_l^{(n)}\int r'\,dr' G_1^{(n)}(r_{k,j}|r')(e^{i\overline{\Omega}_l(r')t} - 1). \tag{A16}$$

Equation (A13) is then solved in terms of normal modes (e.g., eigenmodes of the matrix $A_{k,j;l,i}$) and with a proper definition of the vortex center (e.g., center of a PV contour for which $\eta \equiv 0$). Applying this method to the two-contour case, respectively, in layers k_1 and k_2, with radii r_1, r_2, strengths Δ_1, Δ_2, and where the structure center is defined as the center of the first PV contour (e.g., $\eta_1 \equiv 0$) yields the following equations:

$$-iA_{k1,1;k2,1}\eta_2 = i\frac{\phi_{k1}}{r_1} - (U - U_{k1}) - iV \tag{A17a}$$

$$\frac{\partial}{\partial t}\eta_2 - iA_{k2,1;k2,1}\eta_2 = i\frac{\phi_{k2}}{r_2} - (U - U_{k2}) - iV. \tag{A17b}$$

Subtracting both equations and solving for the PV contour center separation $\eta = \eta_2$ yields using (A16)

$$\eta(t) = i\frac{(U_{k2} - U_{k1})}{\sigma}(1 - e^{i\sigma t}) + \sum_{n,k} -i\beta_k^t\alpha_k^{(n)} \times \int r\,dr\left[\frac{P_{k1}^{(n)}}{r_1}G_1^{(n)}(r_1|r) - \frac{P_{k2}^{(n)}}{r_2}G_1^{(n)}(r_2|r)\right] \times \left[\frac{e^{i\overline{\Omega}_k t} - e^{i\sigma t}}{\overline{\Omega}_k - \sigma} + \frac{1 - e^{i\sigma t}}{\sigma}\right] \tag{A18}$$

with

$$\sigma_1 = A_{k1,1;k2,1} = -\frac{1}{r_1}\sum_n P_{k1}^{(n)}\alpha_{k2}^{(n)}\Delta_2 G_1^{(n)}(r_1|r_2) \tag{A19a}$$

$$\sigma = A_{k2,1;k2,1} - A_{k1,1;k2,1} = -\frac{1}{r_2}\sum_n P_{k2}^{(n)}\alpha_{k1}^{(n)}\Delta_1 G_1^{(n)}(r_2|r_1) - \frac{1}{r_1}\sum_n P_{k1}^{(n)}\alpha_{k2}^{(n)}\Delta_2 G_1^{(n)}(r_1|r_2). \tag{A19b}$$

Using (A18) and (A16) in (A17a) then provides the propagation speed formula (7a)–(7f).

Let us also notice that, to write (7b), we have used the following important integral properties of Bessel functions (see Abramowitz and Stegun 1970)

$$\int r\,dr G_1^{(n)}(r_1|r) = -\frac{r_1}{\gamma_n^2}. \tag{A20}$$

APPENDIX B

Compensation of the Advective Effect

We here prove that the analytic model predicts total compensation of the advective effect by the baroclinic β effect for long time periods. To do so we first show that $\mathbf{u}_\beta$ exactly cancels U_{k1} in (7a).

In (7b) $\mathbf{u}_\beta$ consists of two terms, a constant one and a time-dependent one. Initially they cancel each other, but the contribution of the time-dependent term tends to zero for long time periods because of the oscillating nature of the integrand. Thus, to prove that the $\mathbf{u}_\beta$ exactly cancels U_{k1} for long time period, we have to demonstrate that

$$U_{k1} = \sum_{n,k}\beta_k^U P_{k1}^{(n)}\alpha_k^{(n)}\frac{1}{\gamma_n^2}. \tag{B1}$$

Using the matrices P and α defined in appendix A, we write the Froude matrix associated with the stretching operator Fr = tridiag $[F_k^-, -(F_k^- + F_k^+), F_k^+] = PD\alpha$, where $D = \text{diag}(-\gamma_n^2)$ is a diagonal matrix containing the eigenvalues of Fr. Let us now define a vector $\overline{U}$ whose column contains the component of the current in each layer $(U_1, \ldots, U_N)$. Then the line vector associated with the baroclinic β coefficients can be written

$$\underline{\beta_U} = -(\text{Fr}\overline{U})^t. \tag{B2}$$

Now writing

$$\overline{U} = \text{Fr}^{-1}\,\text{Fr}\,\overline{U} \tag{B3}$$

and transposing yields

$$(\overline{U})^t = (\text{Fr}\,\overline{U})^t(\text{Fr}^{-1})^t \tag{B4}$$

as $\text{Fr}^{-1} = PD^{-1}\alpha$,

$$(\text{Fr}^{-1})^t = \alpha^t D^{-1}P^t \tag{B5}$$

and we get

$$(\overline{U})^t = -\underline{\beta_U}\alpha^t D^{-1}P^t \tag{B6}$$

with $D^{-1} = \text{diag}(-1/\gamma^2)$, which is just (B1) in matrix form. Using the similarity between terms in (7b) and (7c) and the result (A20), it is also possible to show that the last term in (7a) is compensated by the last term in (7c). Thus, advection is compensated by the baroclinic β effect when $t \to \infty$.

The previous results are, strictly speaking, only valid when the Froude matrix Fr is invertible (step B3), that is to say when a barotropic mode does not exist. It seems however possible to generalize the previous calculations by filtering the barotropic part of the current (which only induces a displacement of the whole vortex struc-

ture without affecting its evolution). Steps B3–6 can then be resumed for the baroclinic part of the background current.

Thus, for long time periods, the advective effect found by HS90 and MP93 vanishes because of the development of the baroclinic beta gyres so that the baroclinic current has thus no net effect on the vortex propagation.

REFERENCES

Abramowitz, M., and I. A. Stegun, Eds., 1970: *Handbook of Mathematical Functions.* Appl. Math. Series, Vol. 55, Natl. Bur. of Stand., 231–233.

Armi, L., D. Hebert, N. Oakey, J. F. Price, P. L. Richardson, H. T. Rossby, and B. Ruddick, 1989: Two years in the life of a Mediterranean salt lens. *J. Phys. Oceanogr.,* **10,** 354–370.

Charney, J. G., and M. Stern, 1962: On the instability of internal baroclinic jets in a rotating atmosphere. *J. Atmos. Sci.,* **19,** 159–172.

Chérubin, L., and Coauthors, 1997: Descriptive analysis of the hydrology and currents on the Iberian shelf from Gibraltar to Cape Finisterre: Preliminary results from the SEMANE and INTERAFOS experiments. *Ann. Hydrogr.,* **21,** 5–69.

De Szoeke, R. A., and D. B. Chelton, 1999: The modification of long planetary waves by homogeneous potential vorticity layers. *J. Phys. Oceanogr.,* **29,** 500–511.

Dewar, W. K., 1998: On ''too fast'' baroclinic planetary waves in the general circulation. *J. Phys. Oceanogr.,* **28,** 1739–1758.

——,and G. Flierl, 1987: Some effects of the wind on rings. *J. Phys. Oceanogr.,* **17,** 1653–1667.

Hogg, N., and H. Stommel, 1990: How currents in the upper thermocline could advect meddies deeper down. *Deep-Sea Res.,* **37,** 613–623.

Joyce, T. M., and T. J. McDougall, 1992: Physical structure and temporal evolution of Gulf Stream warm-core ring 82B. *Deep-Sea Res.,* **39,** S19–S44.

Kaz'min, A. S., and G. Sutyrin, 1990: Blocking of the Benguela Current by an isolated anticyclone: Analysis of satellite and shipboard data. *Sov. J. Remote Sens.,* **7,** 986–995.

Marshall, J. S., and B. Parthasarathy, 1993: Tearing of an aligned vortex by a current difference in two-layer quasi-geostrophic flow. *J. Fluid Mech.,* **255,** 157–182.

McWilliams, J., 1985: Submesoscale, coherent vortices in the ocean. *Rev. Geophys.,* **23,** 165–182.

——,and G. Flierl, 1979: On the evolution of isolated, nonlinear vortices. *J. Phys. Oceanogr.,* **9,** 1155–1182.

Morel, Y., 1995a: The influence of an upper thermocline current on intrathermocline eddies. *J. Phys. Oceanogr.,* **25,** 23–51.

——,1995b: Etude des déplacements et de la dynamique des tourbillons géophysiques. Application aux Meddies. Thèse de l'Université Joseph Fourier-Grenoble I, 155 pp. [Available from Y. Morel, EPSHOM-CMO, BP 426, 29275 Brest Cedex, France.]

——, and J. C. McWilliams, 1997: Evolution of isolated interior vortices in the ocean. *J. Phys. Oceanogr.,* **27,** 727–748.

Olson, D. B., 1980: The physical oceanography of two rings observed by the cyclonic ring experiment. Part II: Dynamics. *J. Phys. Oceanogr.,* **10,** 514–528.

——,1991: Rings in the ocean. *Annu. Rev. Earth Planet Sci.,* **19,** 283–311.

——, and R. H. Evans, 1986: Rings of the Agulhas. *Deep-Sea Res.,* **33,** 27–42.

Paillet, J., B. Le Cann, A. Serpette, Y. Morel, and X. Carton, 1999: Real-time tracking of a Galician Meddy. *Geophys. Res. Lett.,* **26,** 1877–1880.

Pedlosky, J., 1987: *Geophysical Fluid Dynamics.* Springer, 710 pp.

Pingree, R. D., and B. Le Cann, 1992: Anticyclonic eddy X91 in the southern bay of Biscay, May 1991 to February 1992. *J. Geophys. Res.,* **97,** 14 353–14 367.

——, and ——, 1993a: Structure of a meddy (Bobby 92) southeast of the Azores. *Deep-Sea Res.,* **40,** 2077–2103.

——, and ——, 1993b: A shallow meddy (a smeddy) from the secondary Mediterranean salinity maximum. *J. Geophys. Res.,* **98,** 20 169–20 185.

——, and ——, 1994: Winter warming in the southern bay of Biscay and Lagrangian eddy kinematics from a deep-drogued argos buoy. *J. Mar. Biol.,* **74,** 107–128.

Reznik, G. M., and W. K. Dewar, 1994: An analytic theory of distributed axisymmetric barotropic vortices on the β-plane. *J. Fluid Mech.,* **269,** 301–321.

Richardson, P., D. Walsh, L. Armi, M. Schröder, and J. F. Price, 1989: Tracking three Meddies with SOFAR floats. *J. Phys. Oceanogr.,* **19,** 371–383.

Sutyrin, G. G., 1987: The beta-effect and the evolution of a localized vortex. *Sov. Phys. Dokl.,* **32,** 791–793.

——, and G. R. Flierl, 1994: Intense vortex motion on the beta-plane: Development of the beta gyres. *J. Atmos. Sci.,* **51,** 773–790.

——, and Y. G. Morel, 1997: Intense vortex motion in a stratified fluid on the beta-plane. An analytical model and its validation. *J. Fluid Mech.,* **336,** 203–220.

van Ballegooyen, R. C., M. L. Grüdlingh, and J. R. E. Lutjeharms, 1994: Eddy fluxes of heat and salt from the southwest Indian Ocean into the southeast Atlantic Ocean: A case study *J. Geophys. Res.,* **99,** 14 053–14 070.

Vandermeirsch, F., 1999: Interaction entre un jet et un tourbillon océanique. Application au courant des Açores et aux Meddies de la campagne SEMAPHORE. Thèse de l'Université de Bretagne Occidentale, 210 pp. [Available from F. Vandermeirsch, EPSHOM-CMO, BP 426, 29275 Brest Cedex, France.]